Remote sensing data processing by multivariate regression analysis method for iron mineral resource potential mapping: A case study in the Sarvian area, central Iran.

Edris Mansouri[1], Faranak Feizi[2*], Alireza Jafari Rad[1], Mehran Arian[1]

1- Department of Geology, Science and Research branch, Islamic Azad University, Tehran, Iran

2- Department of Mining Engineering, South Tehran branch, Islamic Azad University, Tehran, Iran

*corresponding author: Faranak Feizi

Fax number: +98 021 88830012; Cell: +98 912 3006753; faranakfeizi@gmail.com.

ABSTRACT

This paper used multivariate regression to create a mathematical model (with reasonable accuracy) for iron skarn exploration in the region of the interest and generalizing multivariate regression in Mineral Prospectivity Mapping (MPM) field. The main target of this manuscript is to exert multivariate regression analysis (as a MPM method) to iron outcrops mapping from northeast part of the study area to discover new iron deposits in other parts. Two types of multivariate regression models as two linear equations were employed to discover new mineral deposits. The Aster satellite image bands (14 bands) sets as Unique Independent Variables (UIVs) and iron outcrops map as dependent variables were used for MPM. According to the results of p-value, R^2 and R^2_{adj}, the second regression model (which was a multiples and exponents of UIVs) was the fitted model versus other models. Also the accuracy of the model was confirmed by iron outcrops map and geological observations. Based on field observation iron mineralization occurs as contact of limestone and intrusive rocks (skarn type). Iron minerals consist dominantly of magnetite, hematite and goethite.

Key words: Multivariate regression, Mineral Prospectivity Mapping, Iron, Sarvian

1. INTRODUCTION

Preparing the information about an object without touching called remote sensing. The technology of acquiring data through a device which is located at a distance from the object and analysis of the data for interpreting the physical attributes of the object are two facts of remote sensing (Gupta, 2003).Recently, use of remotely-sensed data in natural resources mapping has been popular. In the other words, applications of remote sensing in geological investigations is

the best approach for large scale study (Melesse et al., 2007). In this research, we present some of the most commonly used applications of the techniques in mineral resources mapping.

Diagnosing futuristic zones and finding new mineral deposits in the region of interest, is the definitive main of mineral investigation. One way to achieve this aim is Using satellite image processing for identify Mineral Prospectivity Mapping (MPM) (Carranza, 2008; Abedi et al., 2013; Golshadi et al., 2016 and Feizi et al., 2012).

The utilization of satellite images for mineral investigation has been extremely effective in indicating out the attendance of minerals. Likewise, remote sensing gives the synoptic view, which is useful in distinguishing proof and delineation of different land frames, linear features, and structural elements (Feizi and Mansouri, 2013a).

The regression analysis is a statistical process for estimating the relationships among variables. There are many techniques for analyzing several variables, when the focus is on the relationship between a dependent variable and one or more independent variables, that the latter case, called multivariate regression analysis. This regression analyses have been utilized as a part of numerous logical fields, such as follow geoscience branches.

Identification of stream sediment anomalies have been used by multiple regression analyses (e.g., Carranza, 2010a; Carranza, 2010b). Likewise, multivariate regression has been effectively utilized by Granian et al. (2015) to display subsurface mineralization from lithogeochemical information. Granian et al. (2015) utilized four types of multivariate regression models to depict significant surface geochemical anomalies for acknowledgment subsurface gold mineralization utilizing borehole data as dependent variables and surface lithogeochemical data as independent variables.

Based on previous work such as Allbed et al., (2012), modelling and mapping satellite images data based on regression analysis and remote sensing data is a promising approach, as it facilitates timely detection with a low-cost procedure and allows decision makers to decide what necessary action should be taken in the early stages to Mineral Prospectivity Mapping (MPM) field.

The main objective of this manuscript is to use multivariate regression analysis (as a MPM method) to pixel values of Aster satellite image from north-east part of the study area to identify new iron deposits in other parts. Two types of multivariate regression models utilized to find new mineral deposits, using pixel values of Aster satellite image bands (14 band) sets as Unique Independent Variables (UIVs) and Iron outcrops surface (digitized by geology map of study area (scale 1:5000) and check field) data as dependent variables.

This paper utilized multivariate regression to make a mathematical model (with sensible precision) for iron potential zones investigation in the region of the interest and summing up multivariate regression in remote sensing field.

2. METHODOLOGY

2.1. STUDY AREA

The Sarvian area is located in the Orumieh-Dokhtar magmatic arc in Central of Iran (Fig. 1a). This magmatic arc is the most imperative metallogenic area inside the district and hosts the majority of the larger metals deposits such as lead, zinc, copper and iron (Feizi et al., 2016 and Feizi et al., 2017).

The explored zone determined by Eocene intrusive rocks and carbonates of Qom formation. Several types of metal and non-metal mineral ore deposits have as of now been reported in the study area. According to the 1:100,000 geological map of Kahak, the lithology of this part includes cream limestone with intercalations of marls (Qom formation), dark green, andesitic-basaltic lava, volcanic breccia, hyaloclastic limestone, green megaporphyritic andesitic-basaltic lava, rhyodacitic domes, tonalite-quartzdiorite, microquartzdiorite-microquartzmonzo-diorite, granite-granodiorite, alteration of light green, grey tuff, tuffaceous sandstone and shale with intercalation of nummulitic sandy limestone and andesitic lava, grey limestone, orbitolina bearing, thick bedded to massive (Aptian–Albian) (Feizi et al., 2016) (Fig. 1b).

Figure 1 is about here.

In view of the current confirmations and furthermore contact of intrusive bodies with carbonate rocks (Qom arrangement) and Iron outcrops in the north-east of study area, Calcic iron skarn ore (the Sarvian mine) is located in the northeast of study area (Feizi et al., 2017) (Fig. 2).

Figure 2 is about here.

2.2. MULTIVARIATE REGRESSION

Regression analyses is a good statistical manner for analyzing relationships among variables (Granian et al., 2015). This strategy can show the conduct of an event (a dependent variable) in light of related variables (some independent variables). In regression analyses, if a dependent variable called (Y) and independent variables called (x_i), the equation is:

$$Y = f(x_i). \qquad (1)$$

Y could be linear or non-linear function. For linear regression Y is defined as follows:

$$Y = a_0 + a_1x_1 + a_2x_2 + \cdots + a_ix_i + \varepsilon\,, \quad i = 1,2,\dots,n. \quad (2)$$

For this function, the constant factor is a_0 , the random error is ε , and the regression coefficients are a_i. If there were n samples in a data set, for each sample t variables were measured. Thus, function (2) can be as follows:

$$Y_i = \hat{a}_0 + \hat{a}_1 X_{i1} + \hat{a}_2 X_{i2} + \cdots + \hat{a}_t X_{it} + \varepsilon_i i = 1,2, \dots, n. \qquad (3)$$

Equation (3) can be re-written as a matrix. The linear function matrix is:

$$[Y] = [X][A] + [\varepsilon]. \qquad (4)$$

$$[Y] = \begin{bmatrix} Y_1 \\ Y_2 \\ \cdot \\ : \\ Y_n \end{bmatrix}; \ [A] = \begin{bmatrix} \hat{a}_0 \\ \hat{a}_1 \\ \cdot \\ : \\ \hat{a}_t \end{bmatrix}; [X] = \begin{bmatrix} 1 & X_{11} X_{12} \dots X_{1t} \\ 1 & X_{21} X_{22} \dots X_{2t} \\ & \cdot \\ & : \\ 1 & X_{n1} X_{n2} \dots X_{nt} \end{bmatrix}; \ [\varepsilon] = \begin{bmatrix} \varepsilon_1 \\ \epsilon_2 \\ \cdot \\ : \\ \epsilon_n \end{bmatrix}. \qquad (5)$$

The least squares technique is used for estimating $[A]$ as the coefficient matrix, as follows:

$$[A] = [\sum\ ]^{-1}[C] = ([X]'[X])^{-1}[X]'[Y]. \qquad (6)$$

The inverse of variance-covariance samples matrix is $[\sum\ ]^{-1}$and the covariance matrix among independent variable and samples is$[C]$. Thus by equation 6, the regression coefficients model is calculated.

In regression analysis, some criteria are required to review. These criteria are as follows:

1. The variance and the mean of the random error should be a constant value and zero, respectively.

2. The coefficient of determination value (R^2) should be examined. This value is calculated as follows (Granian et al., 2015):

$$R^2 = \frac{\sum_{i=1}^{n}(\hat{Y}_i - \bar{Y})^2}{\sum_{i=1}^{n}(Y_i - \bar{Y})^2} = 1 - \frac{\sum_{i=1}^{n}(Y_i - \hat{Y}_i)^2}{\sum_{i=1}^{n}(Y_i - \bar{Y})^2}. \quad (7)$$

The mean of the variable ($\bar{Y}$), value of ith sample (Y_i) and estimated value of the ith sample ($\hat{Y}_i$) for dependent variables were used in equation 7. The calculated R^2 value determined within [0, 1] range. The value of R^2 is close to 1 for well fitted models.

1. According to the fact that adding independent variables to the model will increasing R^2 value, the adjusted determination coefficient (R^2_{adj}) is defined as follows (Granian et al., 2015):

$$R^2_{adjusted} = 1 - \frac{n-1}{n-t}(1 - R^2). \quad (8)$$

As it was mentioned, n is number of samples (or data) and t is the number of variables (or regression coefficients). If a set of explanatory variables are introduced into a regression one at a time, with the R^2_{adj}computed each time, the level at which R^2_{adj}reaches a maximum, and decreases afterward, would be a well fitted model.

2. In regression analyses, the model should be fitted to the data. Accordingly, the p-value of the regression model in Analysis of variance (ANOVA) test should be acceptable (less than or equal to 0.05). Also calculating p-value of final coefficients for each model, could help on optimizing and improving the model. This criterion could be considered after choosing the best model.

3. DATA COLLECTION

The iron ore skarn type located in the northeastern of the Sarvian area. There are several iron vein and outcrop in this area. According to the regional geological conditions of the area, the data set of this iron mine is a good model for exploring the surrounding area. In this paper, satellite imagery and map the geology of the mine is used as a training area. In the training area, this method can model the iron outcrops (a dependent variable) based on Aster satellite image bands (some independent variables) (Fig. 3).

Figure 3 is about here.

3.1. REMOTE SENSING DATA (INDEPENDEBT VARIABLES)

The ASTER sensor was propelled in December 1999 on board the Earth Observation System (EOS) US Terra satellite to record sun powered radiation in 14 spectral bands (Table 1). ASTER provides high-resolution images of the land surface, water, ice, and clouds using three separate

sensor subsystems covering 14 multi-spectral bands from visible to thermal infrared. The significant resolution scales are 15m, 30m, and 90m in the visible, short-wave IR, and thermal fR, respectively. ASTER consists of three different subsystems; the Visible and Near Infrared (VNIR), the Shortwave Infrared (SWIR), and the Thermal Infrared (TIR). To find out more about each module click on the item of interest (Feizi and Mansouri, 2013b and Mansouri and Feizi, 2016).

Several factors influence the signal measured at the sensor, for example, float of the sensor radiometric calibration, atmospheric and topographical effects. In this way, Aster data collection was utilized and radiance correlation, such as wavelength, dark subtract and log residual by ENVI5.1 software which is basic for multispectral images, were utilized (Mansouri et al., 2015).

In this study after the corrections, pixels size of SWIR and TIR bands based on VNIR3 band (Panchromatic band) convert to 15 meter, than use layer stacking function to build a new multiband file from georeferenced images of various pixel sizes, extents, and projections.

Table 1 is about here.

3.2. MAPPING OF IRON OUPCROPS (DEPENDENT VARIABLE)

The iron ore skarn type located in the northeastern of the Sarvian area. There are several iron vein and outcrop in this area. In order to mapping of iron outcrops in the training area used from Geological map (1:1000 scale) of iron ore deposit and check field. For preparing of this layer, the shape file layer of iron outcrops convert to raster file with pixel size of 15 meter.

4. RESULTS AND DISCUSSION

Regression analyses needs making proper models. Utilizing multiple, factorial, polynomial and reaction surface regressions have been utilized as a part of numerous logical fields such as geosciences (e.g. Granian et al., 2015). Thus, in this study; Model 1 (Y_1) was generated as a multiple linear regression model and Model 2 (Y_2) was created from Y_1 plus multiplied UIVs. The formulas of two mentioned models are presented in Table 2. So in summary, two linear equations (Y_1 and Y_2) were utilized to discover new mineral deposits, using pixel values of Aster satellite image as independent variables and map of iron outcrops as dependent variables. The models which were proposed in this paper, had become more complexes respectively 1 to 2, model 2 has 106 coefficients (14 for UIVs, 1 as constant, 91 for multiples of UIVs) and model 1 has 15 coefficients (14 for UIVs, 1 as constant, 0 for multiples and exponents of UIVs) (Table 2).
Table 2 is about here.

For assessing the models which are exhibited in Table 2, regression analyses were performed and the critical criteria which are mentioned before, were examined. The values for R^2 , R^2_{adj} and p-value of ANOVA test of 2 multivariate regression models are provided in Table 3.

Table 3 is about here.

Also, Table 4 is presented the calculated coefficients of independent variables in regression models. Other independent variables which are not mentioned in Table 4 were excluded variables. The excluded variables have no effect on the models. This means that, excluded variables didn't have any effect on iron mineralization and behavior of iron outcrop map.

Table 4 is about here.

For distinguishing the best model among 2 models, a few criteria are required to review.

Firstly, the variance and the mean of the random error were acceptable for all of regression models. Secondly, based on Table 4, the p-values of ANOVA test of 2 multivariate regression models were equal to 0. For regression models the acceptable p-value should be less than or equal to 0.05. Thus, this criterion confirmed the validity of models without specifying the most appropriate model.

On the other hand, the value of R^2 is close to 1 for well fitted models. The R^2 values of regression models are presented in Table 3. The lowest R^2 belongs toY_1 and the highest belongs to Y_2. Thus, Y_2 model is better from Y_1 model.

According to the fact that adding independent variables to the model will increasing R^2 value, the R^2_{adj} value should be checked. The R^2_{adj} values of regression models are presented in Table 3. As it was mentioned before, if a set of variables are introduced into a regression, with the R^2_{adj}computed each time, the level at which R^2_{adj}reaches a maximum, and decreases afterward, would be a well fitted model. So, according to Table 3, Y_2 would be the fitted model versus other models. Thus, Y_4 regression model is the most appropriate model for Mineral Prospectivity Mapping.

Thus according to the results of p-value (ANOVA test), R^2 and R^2_{adj}, the Second regression model (Y_2) would be the fitted model versus other models. For generating the mineral prospectivity map the formula of Y_2 was performed in ArcGIS software by raster calculator tool. The normalized mineral prospectivity map of the study area is presented in Fig. 4.

Figure 4 is about here.

To assess the exactness of the selected model, the created prospectivity map was checked by the iron outcrops map in the northeast part of the study area (Fig. 5). The locations of iron outcrops have appropriate adoption with favorable areas of mineral prospectivity map. In addition the adaption of prospectivity map with the iron outcrops in the northeast part of the

study area, three target areas with very high favorability, were checked and the prospectivity map was confirmed by geological observations (Fig. 6). Based on field observation iron mineralization occurs as contact of limestone and intrusive rocks (skarn type). Iron mineralizations consist dominantly of magnetite, hematite and goethite. Therefore, the accuracy of mineral prospectivity map confirmed in the Sarvian area.

Figure 5 is about here.

Figure 6 is about here.

5. CONCLUSION

The conclusions of this manuscript are presented in summary as follows.

1) The regression analysis is an appropriate and direct method for MPM by satellite images data. In this paper, the output of processed satellite image using regression analysis indicates the iron potential zones accurately.

2) The application of multivariate regression analysis (as a MPM method) was confirmed in the Sarvian area. This paper used multivariate regression to create a mathematical model (with reasonable accuracy) for iron mineral exploration in the region of the interest and generalizing multivariate regression in MPM field.

3) Two types of multivariate regression models as two linear equations were employed to discover new mineral deposits. According to the results of p-value, R^2 and R^2_{adj}, the second regression model was the fitted model versus other models.

4) Also the accuracy of the model was confirmed by iron outcrops map and geological observations. Based on field observation iron mineralization occurs contact of limestone and intrusive rocks (skarn type). Iron mineralizations consist dominantly of magnetite, hematite and goethite.

5) The results demonstrate that modelling and mapping satellite images data based on regression analysis and remote sensing data is an efficient approach, as it facilitates timely detection with a low-cost procedure and allows decision makers to decide what necessary action should be taken in the early stages to Mineral Prospectivity Mapping (MPM) field.

6) Regression analysis method is a subset of supervised classification due to the mentioned procedure. In this method, target spectrums of training area are used for modeling and MPM.

ACKNOWLEDGEMENTS

The authors would like to thank Amirabbas KarbalaeiRamezanali for his helpful suggestions.

REFRENCES

Abedi, M., Torabi, S.A. and Norouzi, G.H.: Application of fuzzy AHP method to integrate geophysical data in a prospect scale, a case study: Seridune copper deposit. Bollettino di Geofisica Teorica, 54, 145–164, 2013.

Abrams, M.: The Advanced Spaceborne Thermal Emission and Reflection Radiometer (ASTER): Data products for the high spatial resolution imager on NASA's Terra platform, International Journal of Remote Sensing, 21, 5, 847-859, 2000.

Carranza, E.J.M.: Geochemical anomaly and mineral prospectivity mapping in GIS, Handbook of Exploration Environmental Geochemistry. Elsevier, Amsterdam, 368 p, 2008.

Carranza, E.J.M.: Catchment basin modelling of stream sediment anomalies revisited: incorporation of EDA and fractal analysis. Geochemistry: Exploration, Environment, Analysis, 10, 365–381, 2010a.

Carranza, E.J.M.: Mapping of anomalies in continuous and discrete fields of stream sediment geochemical landscapes. Geochemistry: Exploration, Environment, Analysis, 10, 171–187, 2010b.

Feizi, F. and Mansouri, E.: Identification of Alteration Zones with Using ASTER Data in A Part of Qom Province, Central Iran. Journal of Basic and Applied Scientific Research, 2, 73–84, 2012.

Feizi, F. and Mansouri, E.: Separation of Alteration Zones on ASTER Data and Integration with Drainage Geochemical Maps in Soltanieh, Northern Iran. Open Journal of Geology, 3, 134–142, 2013a.

Feizi, F. and Mansouri, E.: Introducing the Iron Potential Zones Using Remote Sensing Studies in South of Qom Province, Iran. Open Journal of Geology, 3, 278–286, 2013b.

Feizi, F., Mansouri, E. and KarbalaeiRamezanali, A.: Prospecting of Au by Remote Sensing and Geochemical Data Processing Using Fractal Modelling in Shishe-Botagh, Area (NW Iran). Journal of the Indian Society of Remote Sensing, 44, 539–552, 2016.

Feizi, F., KarbalaeiRamezanali, A. and Mansouri, E.: Calcic iron skarn prospectivity mapping based on fuzzy AHP method, a case Study in Varan area, Markazi province, Iran. Geosciences Journal, 21, 123–136, 2017.

Granian, H., Tabatabaei, S. H., Asadi, H. H. and Carranza, E. J. M.: Multivariate regression analysis of lithogeochemical data to model subsurface mineralization: a case study from the Sari Gunay epithermal gold deposit, NW Iran. Journal of Geochemical Exploration, 148, 249–258, 2015.

Golshadi, Z., KarbalaeiRamezanali, A. and Kafaei, K.: Interpretation of magnetic data in the Chenar-e Olya area of Asadabad, Hamedan, Iran, using analytic signal, Euler deconvolution, horizontal gradient and tilt derivative methods. Bollettino di Geofisica Teorica ed Applicata, 57, 329–342, 2016.

Gupta, R. P.: Remote sensing geology, Berlin, Heidelberg: Springer Berlin Heidelberg: Imprint: Springer, 2003.

Allbed, A., Kumar, L., and Sinha, P.: Mapping and Modelling Spatial Variation in Soil Salinity in the Al Hassa Oasis Based on Remote Sensing Indicators and Regression Techniques, Remote Sens. 6, 1137-1157; 2014.

Mansouri, E., Feizi, F. and KarbalaeiRamezanali, A.: Identification of magnetic anomalies based on ground magnetic data analysis using multifractal modelling: a case study in Qoja-Kandi, East Azerbaijan Province, Iran. Nonlinear Processes in Geophysics, 22, 579–587, 2015.

Mansouri, E., Feizi, F.: Introducing Au potential areas, using remote sensing and geochemical data processing using fractal method in Chartagh, western Azarbijan – Iran, E. Archive of Mining Sciences, Vol., No 2, 397–414, 2016.

Melesse, A. M., Weng, Q., Thenkabail, P. S. and Senay, G. B.: Remote Sensing Sensors and Applications in Environmental Resources Mapping and Modelling, Sensors, 7, 3209-3241, 2007.

Table 1. Wavelength ranges and spatial resolutions of ASTER bands (Abrams, 2000).

Module	VNIR	SWIR	TIR
Spectral bandwidth (µm)	Band 1 0.52 - 0.60	Band 4 1.650 - 1.700	Band 10 8.125 - 8.475
	Band 2 0.63 - 0.69	Band 5 2.145 - 2.185	Band 11 8.475 - 8.825
	Band 3 N 0.78 - 0.86	Band 6 2.185 - 2.225	Band 12 8.925 - 9.275
	Band 3 B 0.78 - 0.86 (backward looking)	Band 7 2.235 - 2.285	Band 13 10.25 - 10.95
		Band 8 2.295 - 2.395	Band 14 10.95 - 11.65
		Band 9 2.360 - 2.430	
Spatial resolution (m)	15	30	90

Table2. Formula of regression models used for Aster satellite image bands

Types of Regression	Number of coefficients	Formula
First-Degree	15	$Y_1 = a_0 + a_1x_1 + a_2x_2 + \cdots + a_{14}x_{14}$
First-Degree	106	$Y_2 = Y_1 + a_{15}x_1x_2 + a_{16}x_1x_3 + \cdots + a_{27}x_1x_{14} + a_{28}x_2x_3 + a_{29}x_2x_4 + \cdots + a_{39}x_2x_{14} + a_{40}x_3x_4 + a_{41}x_3x_5 + \cdots + a_{50}x_3x_{14} + a_{51}x_4x_5 + \cdots + a_{60}x_4x_{14} + a_{61}x_5x_6 + \cdots + a_{69}x_5x_{14} + a_{70}x_6x_7 + \cdots + a_{77}x_6x_{14} + a_{78}x_7x_8 + \cdots + a_{84}x_7x_{14} + a_{85}x_8x_9 + \cdots + a_{90}x_8x_{14} + a_{91}x_9x_{10} + \cdots + a_{96}x_9x_{14} + a_{97}x_{10}x_{11} + \cdots + a_{100}x_{10}x_{14} + a_{101}x_{11}x_{12+\cdots+}a_{103}x_{11}x_{14} + a_{104}x_{12}x_{13} + a_{105}x_{12}x_{14} + a_{106}x_{13}x_{14}$

Table 3. The values for R^2 , $R^2_{adj}$and p-value of ANOVA test of 2 multivariate regression models

Models	R^2	R^2_{adj}	p-value (ANOVA)
Y_1	0.738	0.715	0
Y_2	0.847	0.829	0

Table 4. The calculated coefficients of regression models 1 and 2.

Model 1		**Model 2**	
variables	Coefficients (a_i)	variables	Coefficients (a_i)
CST	0.275	CST	0.677
$\boldsymbol{x_1}$	-0.01	x_1	-0.014
$\boldsymbol{x_2}$	-0.12	x_2	-0.019
$\boldsymbol{x_3}$	-0.019	x_3	-0.045
$\boldsymbol{x_4}$	0.003	x_4	0.022
$\boldsymbol{x_5}$	-0.006	x_5	-0.017
$\boldsymbol{x_6}$	-0.005	x_6	-0.001
$\boldsymbol{x_7}$	-	x_7	-
$\boldsymbol{x_8}$	-0.004	$\boldsymbol{x_8}$	-0.02
$\boldsymbol{x_9}$	-0.005	$\boldsymbol{x_9}$	-0.006
$\boldsymbol{x_{10}}$	0.009	$\boldsymbol{x_{10}}$	-0.014
$\boldsymbol{x_{11}}$	0.005	$\boldsymbol{x_{11}}$	0.024
$\boldsymbol{x_{12}}$	0.016	$\boldsymbol{x_{12}}$	0.024
$\boldsymbol{x_{13}}$	0.002	$\boldsymbol{x_{13}}$	0.018
$\boldsymbol{x_{14}}$	0.022	$\boldsymbol{x_{14}}$	0.036
-	-	x_1x_4	-0.0009
-	-	x_1x_6	-0.0002
-	-	x_4x_9	-0.0009
-	-	x_7x_8	0.00082

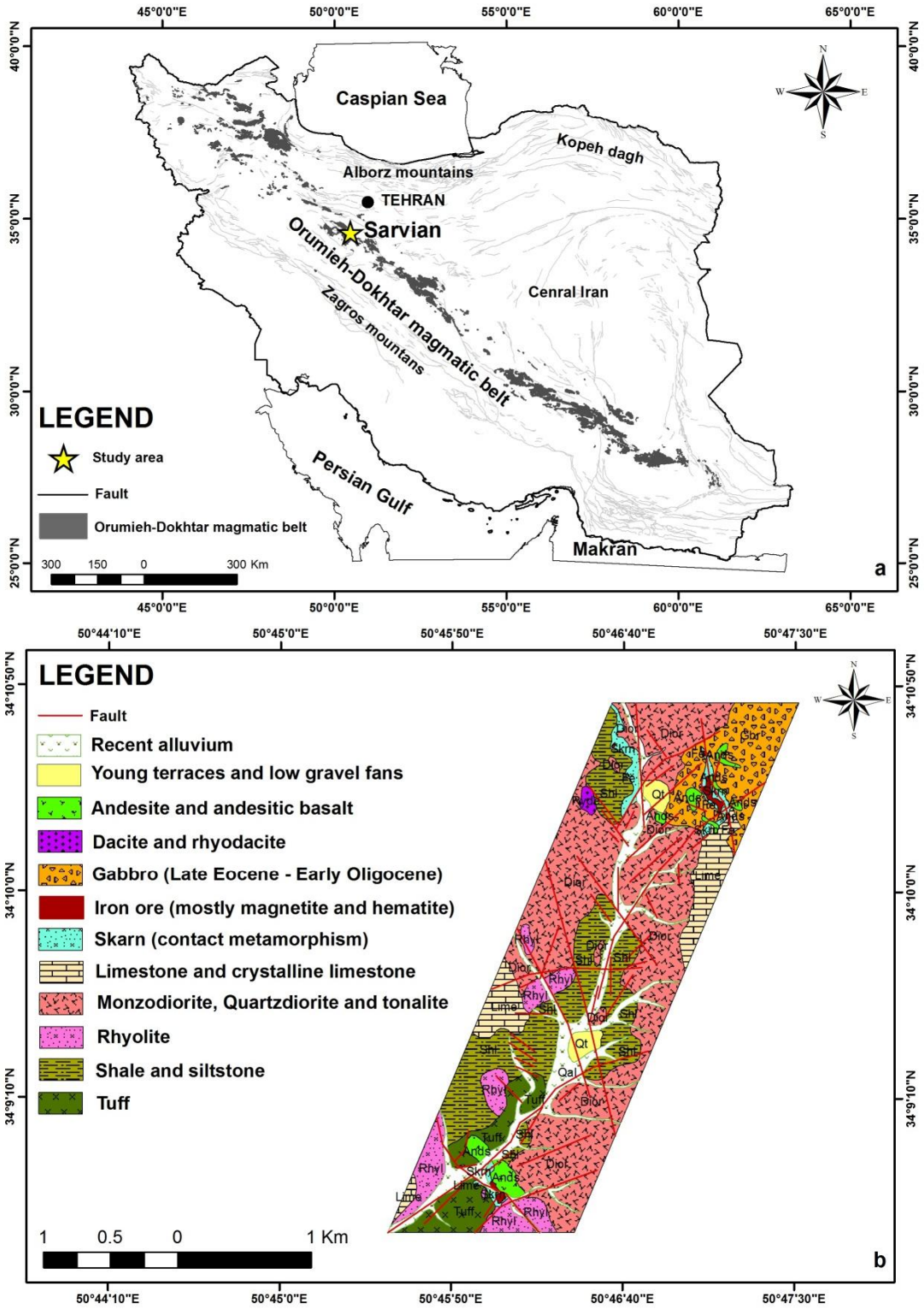

Fig. 1. a) The location of the Sarvian area in the Orumieh–Dokhtar magmatic belt, Iran **b)** Geological map of the Sarvian area (scale 1:25000).

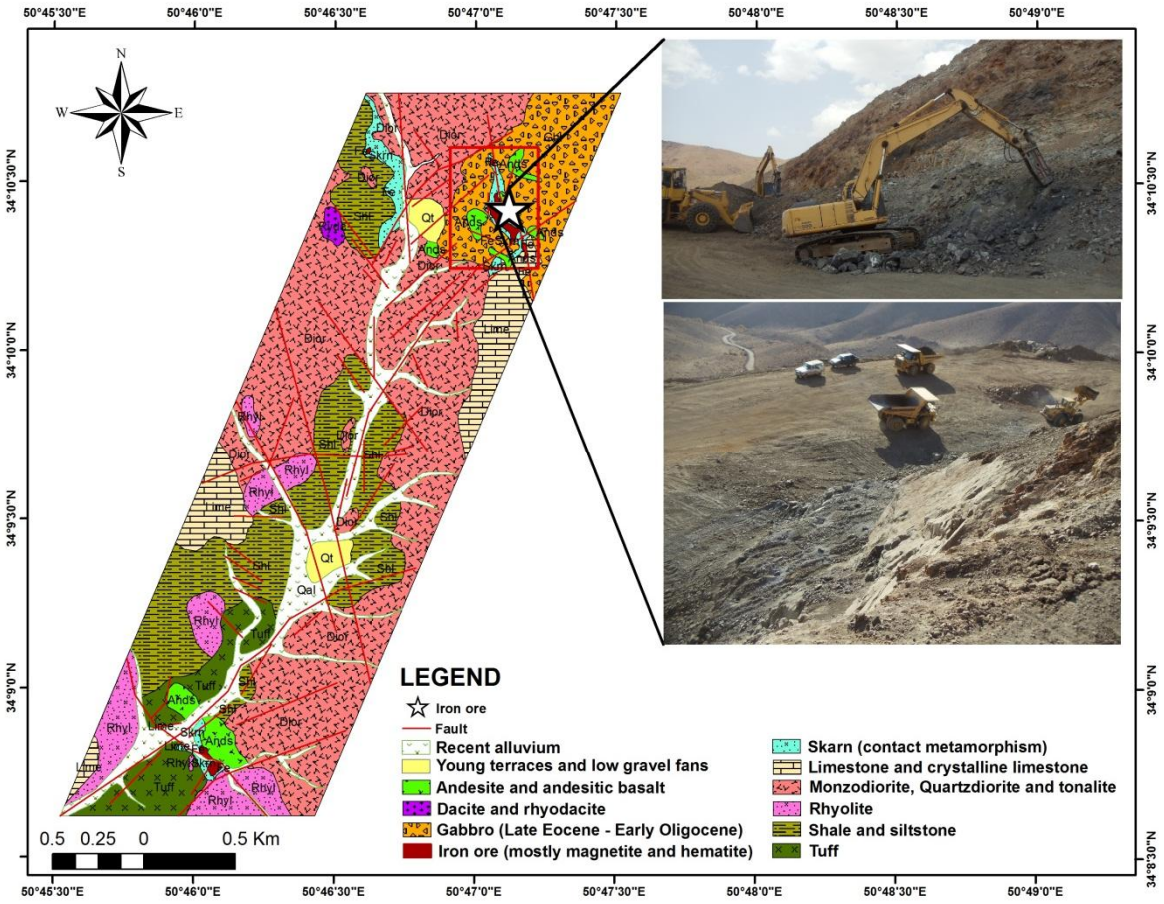

Fig. 2. Location of the Sarvian iron mine in the study area.

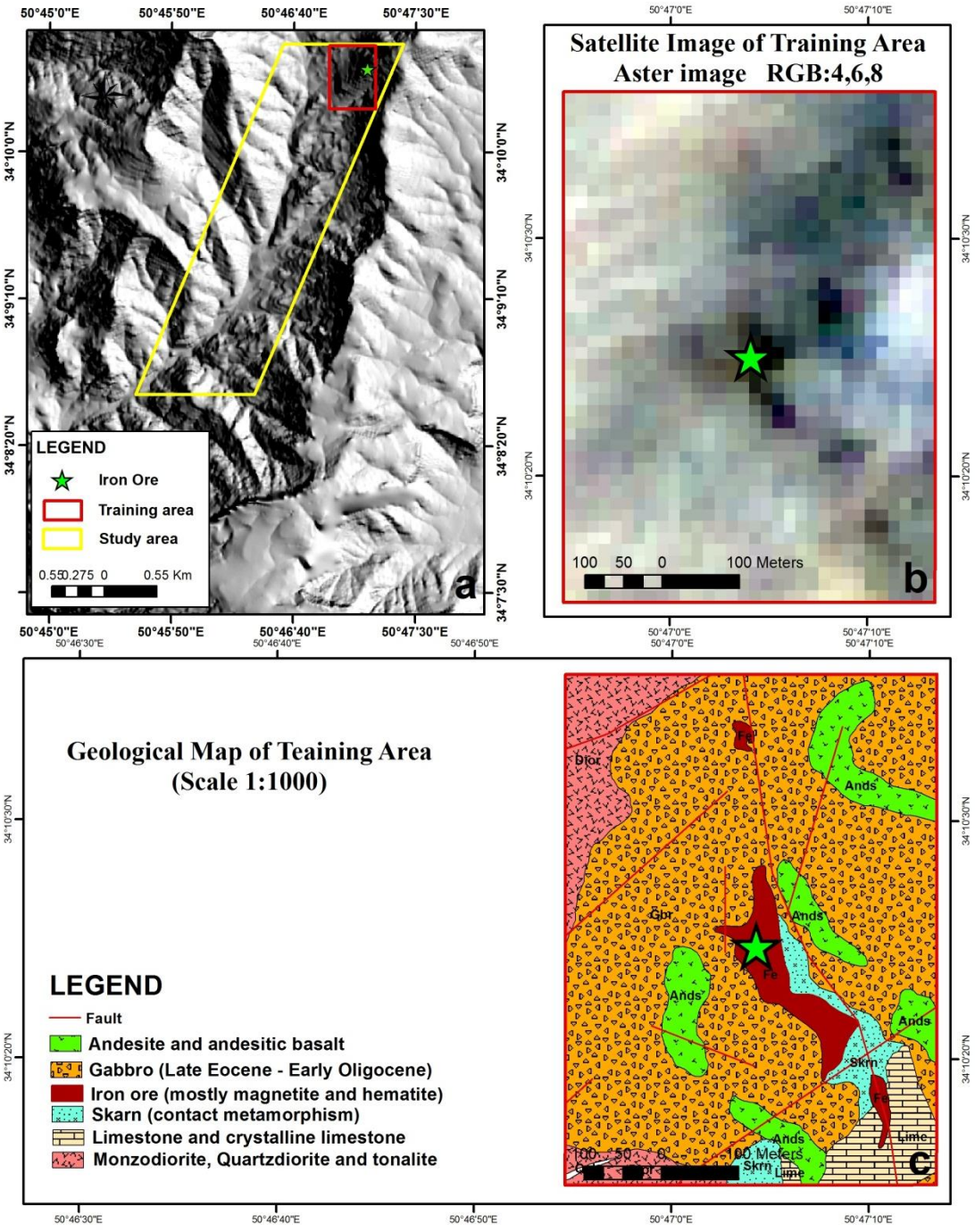

Fig. 3. a) Location of training area in the study area. b) Aster satellite image in the training area (RGB:4,6,8). c) Geological map (scale 1:1000) of training area.

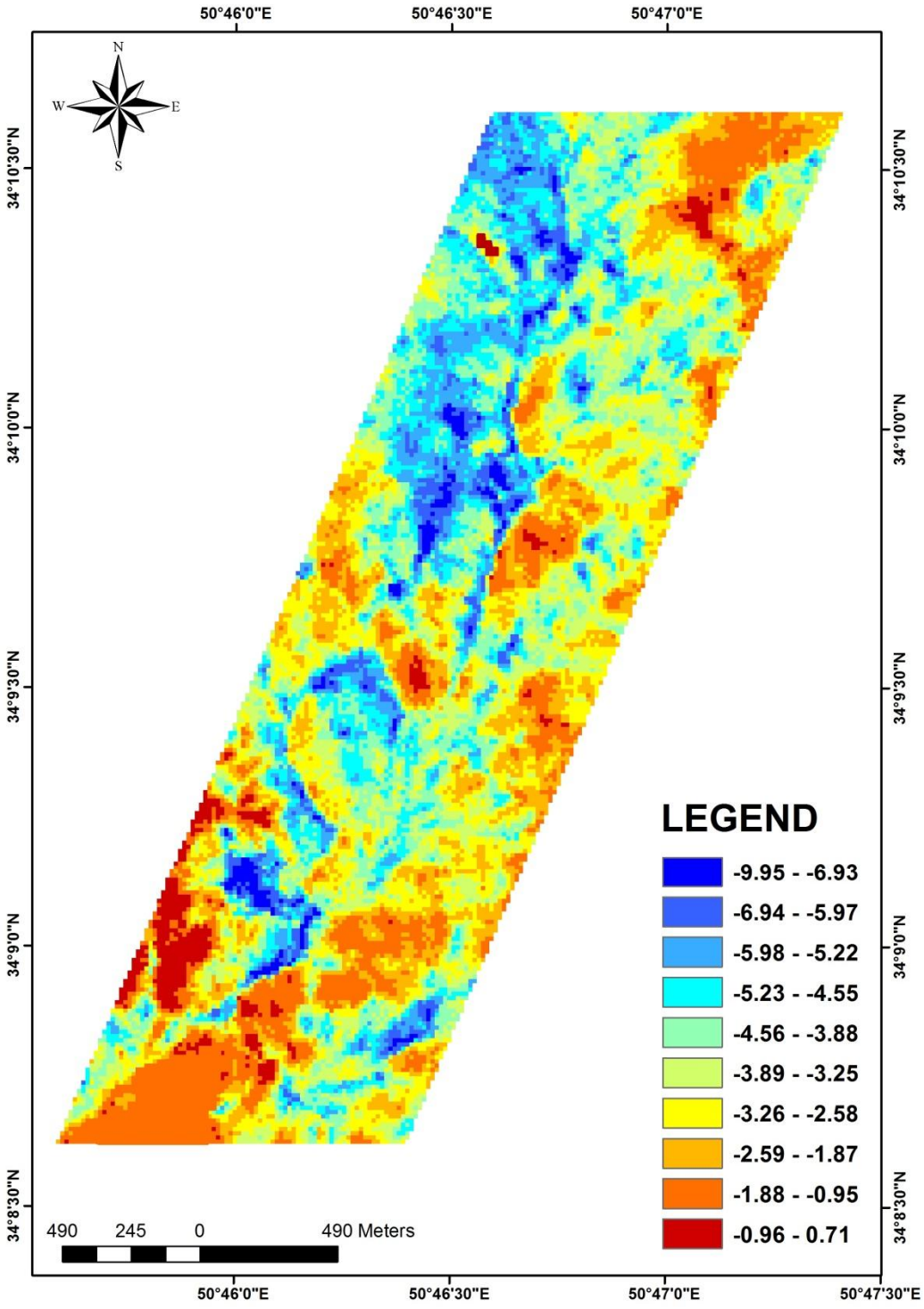

Fig. 4. Mineral prospectivity map of the Sarvian area.

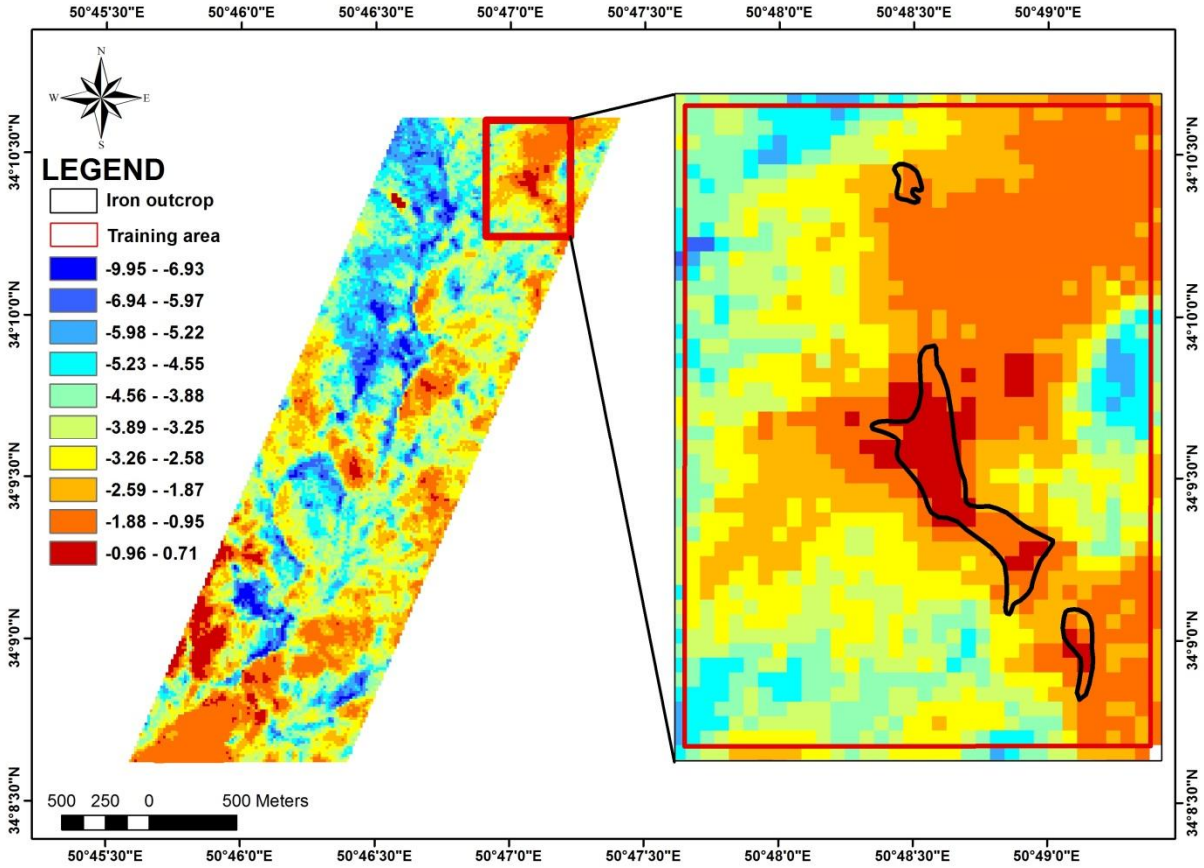

Fig. 5. Mineral prospectivity map of the Sarvian area which confirmed by iron outcrops.

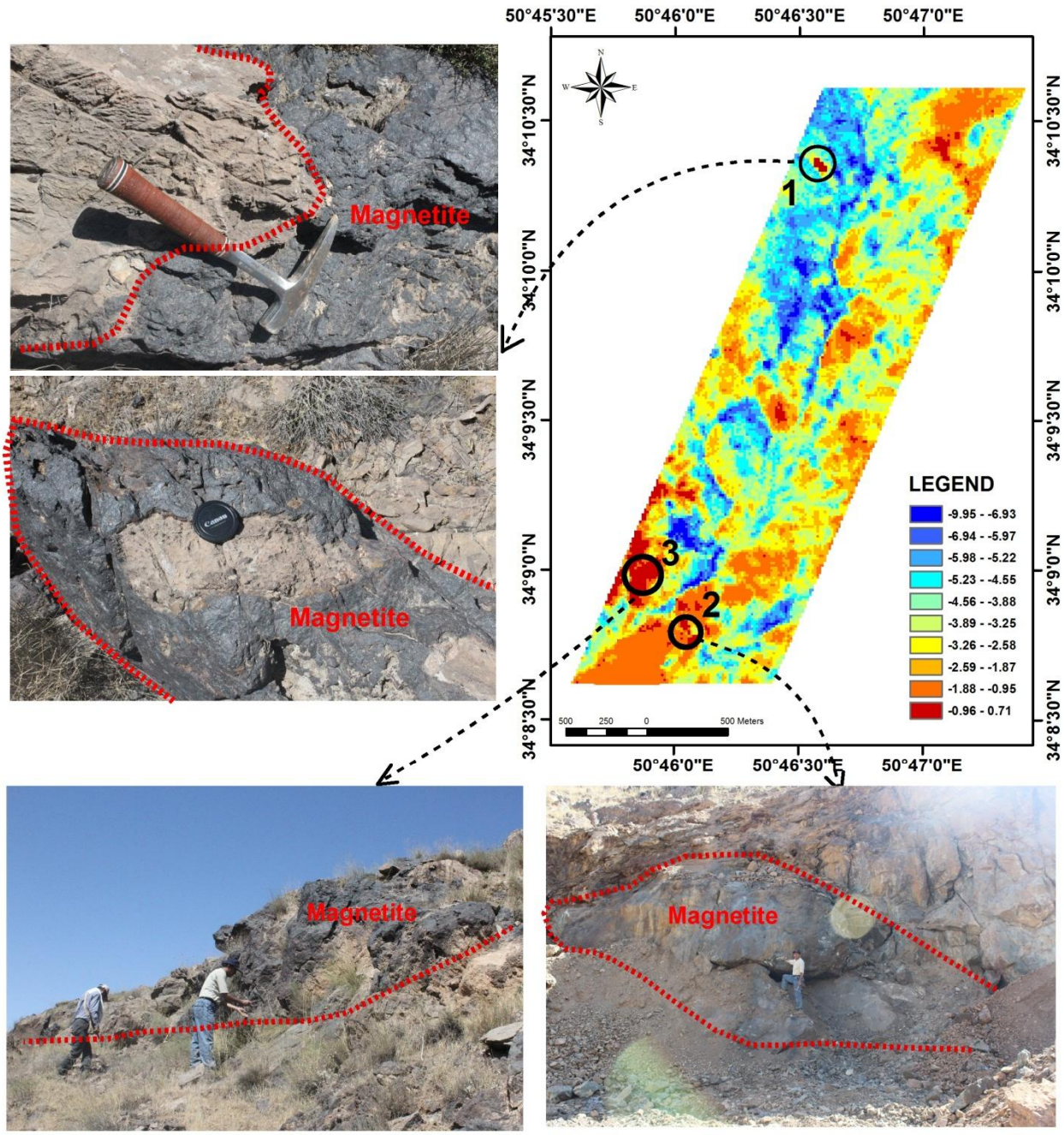

Fig. 6. Mineral prospectivity map of the Sarvian area which confirmed by check field of three target areas.